The $C_5H_6NH_2^+$ Protonated Shiff Base: An *ab Initio* Minimal Model for Retinal Photoisomerization

M. Garavelli,[†] P. Celani,[‡] F. Bernardi,*[,†] M. A. Robb,*[,‡] and M. Olivucci*[,†]

Contribution from the Dipartimento di Chimica "G. Ciamician", Universitá di Bologna, via Selmi n. 2, Bologna I-40126, Italy, and Department of Chemistry, King's College London, Strand, London, WC2R 2LS, United Kingdom

Received April 2, 1996. Revised Manuscript Received April 22, 1997[⊗]

Abstract: The minimum energy path for photoisomerization of the *minimal* retinal protonated Shiff base model *tZt*-penta-3,5-dieniminium cation (*cis*-$C_5H_6NH_2^+$) is computed using MC−SCF and multireference Møller−Plesset methods. The results show that, upon excitation to the spectroscopic state, this molecule undergoes a *barrierless* relaxation toward a configuration where the excited and ground states are *conically intersecting*. The intersection point has a ∼80° twisted central double bond which provides a route for fully efficient nonadiabatic *cis* → *trans* isomerization. This mechanism suggests that *cis*-$C_5H_6NH_2^+$ provides a suitable "*ab initio*" model for rationalizing the observed "ultrafast" (sub-picosecond) isomerization dynamics of the retinal chromophore in rhodopsin. The detailed analysis of the computed reaction coordinate provides information on the changes in molecular structure and charge distribution along the isomerization path. It is shown that the initial excited state motion is dominated by stretching modes which result in an elongation of the central double bond of the molecule associated with the change in bond order in the excited state. Thus, the actual *cis* → *trans* isomerization motion is induced only after the bond stretching has been completed. It is also demonstrated that, along the excited state isomerization coordinate, the positive charge is progressively transferred from the -CH−CH=NH_2 to the CH_2=CH−CH- molecular fragment. Thus, at the intersection point, the charge is completely localized on the CH_2=CH−CH- fragment. This result suggests that strategically placed counterions can greatly affect the rate, specificity, and quantum yield of the photoisomerization.

1. Introduction

The photoisomerization of the retinal chromophore triggers the conformational changes underlying the activity of rhodopsin proteins.[1] In rhodopsin itself, the retinal molecule is embedded in a hydrophobic cavity where it is covalently bound to a lysine residue via a protonated Shiff base (PSB) linkage. The absorption of a photon of light causes the isomerization of the 11-*cis* isomer of the retinal protonated Shiff base (PSB11) to its *all-trans* isomer (PSBT).

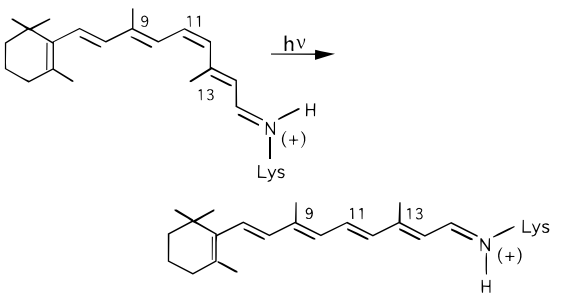

(1)

Recently, femtosecond pump−probe experiments have shed light on the dynamics of PSB11 isomerization both in the protein[2,3] and in solution.[4] The isomerization reaction is apparently concurrent with an extremely efficient excited state radiationless deactivation and is completed on the sub-picosecond (in the protein) or picosecond (in solution) time scale. A similar time scale has been observed for the PSBT[5,6] and PSB13[5] chromophores in solution. The nature of the sub-picosecond isomerization motion in rhodopsin has been investigated by Mathies and Peteanu et al.[2] They observe coherent vibrational motion in the population of nascent PSBT comprising 60 cm^{-1} oscillations. This finding is indicative of nonadiabatic motion along a coordinate leading from excited state PSB11 to ground state PSBT within a single vibrational oscillation. Such motion can only occur if the isomerization coordinate on the excited state *continues directly* onto the ground state potential energy surface thus avoiding excited state equilibration. More recently, Shichida et al.[3] have provided detailed information on the excited state dynamics of rhodopsin. On the basis of transient absorption spectra, it has been proposed that during the first 25 fs the excited state PSB11 chromophore moves out of the Franck−Condon (FC) region along a mode which involves mainly the stretching of the polyene chain. After this initial motion, PSB11 relaxes along a different coordinate and reaches a lower lying S_1 region where S_1 to S_0 decay occurs within 60 fs. The conjecture that the initial motion out of the FC region does not involve substantial torsion has also been suggested by Ottolenghi and Sheves et al.[7] and Hochstrasser[8] for bacteriorhodopsin.

The rationalization of these observations requires a detailed knowledge of the force field providing the driving force for the

[†] Universitá di Bologna via Selmi 2.

[‡] King's College London Strand.

[⊗] Abstract published in *Advance ACS Abstracts,* June 15, 1997.

(1) Yoshizawa, T.; Kuwata, O. In *CRC Handbook of Organic Photochemistry and Photobiology*; Horspool, W. M., Song, P.-S., Ed.; CRC Press: Boca Raton, FL, 1995; pp 1493−1499.

(2) (a) Schoenlein, R. W.; Peteanu, L. A.; Mathies, R. A.; Shank C. V. *Science* **1991**, *254*, 412−415. (b) Wang, Q.; Schoenlein, R. W.; Peteanu, L. A.; Mathies, R. A.; Shank, C. V. *Science* **1994**, *266*, 422−424.

(3) (a) Kandori, H.; Sasabe, H.; Nakanishi, K.; Yoshizawa, T.; Mizukami, T.; Shichida, Y. *J. Am. Chem. Soc.* **1996**, *118*, 1002, 1005. (b) Mizukami, T.; Kandori, H.; Shichida, Y.; Chen, A.-H.; Derguini, F.; Caldwell, C. G.; Bigge, C. Y.; Nakanishi, K.; Yoshizawa, T. *Proc. Natl. Acad. Sci. U.S.A.* **1993**, *90*, 4072−4076.

(4) Kandori, H.; Katsuta, Y.; Ito, M.; Sasabe, H. *J. Am. Chem. Soc.* **1995**, *117*, 2669−2670.

(5) Logunov, S. L.; Song, L.; El-Sayed, M. *J. Phys. Chem.* **1996**, *100*, 18586−18591.

(6) Hamm, P.; Zurek, M.; Röschinger, T.; Patzelt, H.; Oesterhelt, D.; Zinth, W. *Chem. Phys. Lett.* **1996**, *263*, 613−621.

S0002-7863(96)01089-X CCC: $14.00

isomerization process. This force field can be conveniently discussed in terms of excited and ground state potential energy surfaces of the chromophore along the isomerization coordinate. During the last few years, significant progress in the computation of the excited states of *isolated* molecules has been achieved. In particular, it has been demonstrated that the excited state energetics of sizable polyenes (from butadiene to octatetraene) can be computed with reasonable accuracy using high-level *ab initio* quantum chemical methodologies.[9] Furthermore, in a recent paper, we have demonstrated that computed excited state minimum energy paths (MEP) and reaction barriers for radiationless deactivation and *trans* → *cis* isomerization of a series of polyenes are in good agreement with the available experimental data.[10] Thus, in this report, high-level *ab initio* computations (MC−SCF[11a] and multireference Møller−Plesset perturbation theory[12a]) are used to investigate the photoisomerization MEP and the changes in excited state charge distribution of the *minimal* retinal model *tZt*-penta-3,5-dieniminium cation in isolated conditions and in absence of a counterion.

While the actual dynamics of PSBs must depend on the chain length, the counterion, and the surrounding environment (e.g., in rhodopsin PSB11 photoisomerization is faster[3,4] and has a higher quantum yield[13] than in solution), the *ab initio* computation of the photoisomerization path of a simple triene PSB cation has never been presented before. Here, the *tZt*-penta-3,5-dieniminium cation is taken as PSB11 model. In fact, despite its limited size, the *tZt*-penta-3,5-dieniminium cation (*cis*-C_5H_6-NH_2^+) features a "central" *cis* double bond comprised between a polyene (H_2C═CH-) and a polyeniminium (-CH═NH_2^+) residues. Thus *cis*-$C_5H_6NH_2^+$ can be seen as the simplest possible (i.e., minimal) model for PSB11 where the "central" 11-*cis* double bond is located between a butadienyl (ionone−HC═CH−CH═CH-) and a propeniminium (-CH═CH−CH═NH_2^+) conjugating residues (the bulky ionone ring is twisted with respect to the molecular plane[14] and the double bond is only partially conjugated with the rest of the polyene chain).

High-level *ab initio* quantum chemical studies of the parent PSB11 have been limited to computations of the excitation energies. Davidson et al.,[15] using MRSD−CI computations, predict that the first excited state in the FC region of PSB11 is the ionic, spectroscopically allowed, ^1B_u-like state (in this work we use symmetry labels B_u and A_g to refer to the analogy with the electronic states of the corresponding *all-trans* polyene). Davidson and co-workers have also investigated the short-chain homologues, the methaniminium (CH_2═NH_2^+) and propeniminium (CH_2═CH−CH═NH_2^+) cations.[16] Again, the ^1B_u-like ionic state has been found to correspond to the first excited state. More recently these results have been confirmed by Martin[17] who has also computed, using a semiempirical effective Hamiltonian technique, the excitation energies for a series of *all-trans* PSB going from the methaniminium to the undeca-3,5,7,9,11-penteniminium cation. *Ab initio* investigations of the photoisomerization process of short-chain PSB cations along *assumed* reaction coordinates has been carried out by Bonacic-Koutecky and Michl et al.[18] and, more recently, by Nonella et al.[19] using *ab initio* MRD−CI and MRSD−CI computations, respectively. For the methaniminium cation, Bonacic-Koutecky and Michl et al.[18] found a conical intersection between the S_1 and ground state energy surfaces at a 90° twisted configuration. However, for the longer prop-3-eniminium cation, this feature was not documented.[18b] Nonella et al. investigated the structure of the S_1 and S_0 potential energy surfaces along two adjacent torsions (about the $C_\beta-C_\gamma$ and $C_\alpha-C_\beta$ bonds) for the *all-trans*-penta-3,5-dieniminium cation (*trans*-$C_5H_6NH_2^+$), but no S_1/S_0 intersection was found. Such computations appear to agree with the results of earlier semiempirical studies by Dormans,[20] where it was found that the ionic ^1B_u-like state is the lowest excited state along the assumed reaction coordinate.

The computer modeling of the *cis* → *trans* isomerization dynamics of PSB11 and PSBT embedded in the corresponding proteins rhodopsin and bacteriorhodopsin is a "grand challenge" problem. Given the exceptionally high cost of accurate computations, past work in this area has relayed on reaction potential energy surfaces computed at the QCFF/PI[21] and semiempirical levels of theory.[22,23] These energy surfaces suggest that after photoexcitation the PSB11 reaches a twisted excited state intermediate, where thermal equilibration is approached, and decay to the ground state occurs via internal conversion according to the Fermi Golden rule. However, Warshel and Weiss[21a] were the first to suggest that an *unusually large* decay probability, which prevents excited state equilibration, is required to explain the observed high quantum yield and short reaction time in rhodopsin photoisomerization. More recently, on the basis of the experimental evidence, Mathies et al.[2] suggested that the extremely fast isomerization of PSB11 in rhodopsin can be explained by a Landau−Zener[24] dynamical internal conversion process. The presence of a conical intersec-

(7) Delaney, J. K.; Brack, T. L.; Atkinson, G. H.; Ottolenghi, M.; Steinberg, G.; Sheves, M. *Proc. Natl. Acad. Sci. U.S.A.* **1995**, *90*, 2101−2105.

(8) Haran, G.; Wynne, K.; Xie, A.; He, Q.; Chance, M.; Hochstasser, R. M. *Chem. Phys. Lett.* **1996**, 389−395.

(9) Serrano-Andrés, L.; Lindh, R.; Roos, B. O.; Merchán, M. *J. Phys. Chem.* **1993**, *97*, 9360−9368.

(10) Celani, P.; Garavelli, M.; Ottani, S.; Bernardi, F.; Robb, M. A.; Olivucci, M. *J. Am. Chem. Soc.* **1995**, *117*, 11584−11585.

(11) (a) Roos, B. O. *Adv. Chem. Phys.* **1987**, *69*, 399−446. (b) The MC−SCF program used is implemented in the following: *Gaussian 94*, Revision B.2; Frisch, M. J.; Trucks, G. W.; Schlegel, H. B.; Gill, P. M. W.; Johnson, B. G.; Robb, M. A.; Cheeseman, J. R.; Keith, T.; Petersson, G. A.; Montgomery, J. A.; Raghavachari, K.; Al-Laham, M. A.; Zakrzewski, V. G.; Ortiz, J. V.; Foresman, J. B.; Peng, C. Y.; Ayala, P. Y.; Chen, W.; Wong, M. W.; Andres, J. L.; Replogle, E. S.; Gomperts, R.; Martin, R. L.; Fox, D. J.; Binkley, J. S.; Defrees, D. J.; Baker, J.; Stewart, J. P.; Head-Gordon, M.; Gonzalez, C.; Pople, J. A. Gaussian, Inc.: Pittsburgh, PA, 1995.

(12) (a) Andersson, K.; Malmqvist, P.-A.; Ross, B. O. *J. Chem. Phys.* **1992**, *96*, 1218. (b) *MOLCAS*, Version 3; Andersson, K.; Blomberg, M. R. A.; Fülscher, M.; Kellö, V.; Lindh, R.; Malmqvist, P.-A.; Noga, J.; Olsen, J.; Roos, B. O.; Sadlej, A. J.; Siegbahn, P. E. M.; Urban, M.; Widmark, P. O.; University of Lund, Sweden, 1994.

(13) Freedman, K. A.; Becker, R. S. *J. Am. Chem. Soc.* **1986**, *108*, 1245−1251.

(14) There is no general agreement on the value of this twisting angle of the 11-*cis*-retinal chromophore. In this molecule, the *β*-ionone ring is assumed to be 6-s-*cis*. For this conformation, Sakurai et al. (Sakurai, M.; Wada, M.; Inoue, Y.; Tamura, Y.; Watanabe, Y. *J. Phys. Chem.* **1996**, *100*, 1957−1964) give a value of 59°. Davidson et al. take a value of 57−58° (see ref 15). An estimate based upon a partial b3lyp/6-31-G* geometry optimization gives a 30° angle.

(15) Du, P.; Davidson, E. R. *J. Phys. Chem.* **1990**, *94*, 7013−7020.

(16) Du, P.; Racine, C.; Davidson, E. R. *J. Phys. Chem.* **1990**, *94*, 3944−3951.

(17) (a) Martin, C. H. *J. Phys. Chem.* **1996**, *100*, 14310−14315. (b) Martin, C. H. *Chem. Phys. Lett.* **1996**, *257*, 229−237.

(18) (a) Bonacic-Koutecky, V.; Köhler, J.; Michl, J. *Chem. Phys. Lett.* **1984**, *104*, 440−443. (b) Bonacic-Koutecky, V.; Schöffel, K.; Michl, J. *Theor. Chim. Acta* **1987**, *72*, 459−474.

(19) Dobado, J. A.; Nonella, M. *J. Phys. Chem.* **1996**, *100*, 18282−18288.

(20) Dormans, G. J.; Groenenboom, G. C.; van Dorst, W. C. A.; Buck, H. M. *J. Am. Chem. Soc.* **1988**, *110*, 1406−1415.

(21) (a) Weiss, R. M.; Warshel, A. *J. Am. Chem. Soc.* **1979**, *101*, 6131−6133. (b) Warshel, A.; Barboy, N. *J. Am. Chem. Soc.* **1982**, *104*, 1469−1476.

(22) Birge, R. R.; Hubbard, L. M. *J. Am. Chem. Soc.* **1980**, *102*, 2195−2205.

(23) Humphrey, W.; Xu, D.; Sheves, M.; Schulten, K. *J. Phys. Chem.* **1995**, *99*, 14549−14560.

(24) (a) Landau, L. D. *Phys. Z. Sowjetunion* **1932**, *2*, 46. (b) Zener, C. *Proc. R. Soc. London, Ser. A* **1932**, *137*, 696.

tion[25] (i.e., a real crossing) between the S_1 and S_0 potential energy surfaces of PSB11 and located at the end of a S_1 relaxation path would provide a clear-cut explanation of the extreme velocity of such radiationless decay. While the involvement of a conical intersection in the photoisomerization of PSB11 has been suggested before,[18] no direct computational evidence of this feature has been reported even for a minimal triene model (e.g., this feature has not been documented by either *ab initio*[18,19] or semiempirical[17] computations).

Effective computational tools and strategies for the search and characterization of excited state reaction paths and conical intersections in sizable organic molecules are now available (see ref 26 for a recent review). The reaction coordinate does not need to be assumed; rather it can be unambiguously determined. In this paper, the *cis*-$C_5H_6NH_2^+$ *cis* → *trans* reaction coordinate is computed at the *ab initio* MC−SCF level of theory by computing the MEP connecting the FC region to the ground state photoproduct valley. These computations make use of a novel technique[27] to follow the steepest descent path from regions like the FC region on the S_1 energy surface or conical intersection points on the S_0 energy surface. The energetics along the resulting MEP are then accurately determined using multireference Møller−Plesset perturbation theory.[12]

The central result of our study to be discussed in this paper is that, upon excitation to the spectroscopic state (S_1), *cis*-$C_5H_6NH_2^+$ undergoes a *barrierless* relaxation toward a configuration where the S_1 and S_0 energy surfaces are *conically intersecting*. The intersection point has a ∼80° twisted central double bond which provides a route for fully efficient nonadiabatic *cis* → *trans* isomerization. In addition, our computations provide a quantitative picture of the evolution of the bonding and charge distribution along the photoisomerization path of the model system. During S_1 motion, the positive charge migrates and localizes on the CH_2CHCH- moiety. In the vicinity of the intersection point, the S_1 and S_0 charge distributions are related by a *net one-electron transfer* between the two rotated halves of the molecule (i.e., between the CH_2CHCH- and -$CHCHNH_2$ moieties).

2. Computational Methods

All MC−SCF energy and gradient computations have been carried out using a complete active space (CAS) with the 6-31+G* basis set available in *Gaussian 94*.[11b] The S_0 *cis* and *trans* minima and the S_0 MEPs have been computed using a CAS with six electrons in six π orbitals. The S_1 MEP has been computed using state-averaged orbitals in order to avoid MC−SCF convergence failure. To correct for the loss in accuracy due to the use of state-averaged orbitals, we have used an augmented six electrons in nine π orbitals CAS. (In order to limit the cost of these computations, we have used the 6-31G* basis set for evaluating the reaction coordinate. Geometry optimizations on S_1 *cis*-$C_5H_6NH_2^+$ and shorter PSB demonstrate that the two basis sets yield the same geometrical parameters.) In order to improve the energetics by including the effect of dynamic electron correlation, the MC−SCF/6-31+G* energies have been recomputed at the multireference Møller−Plesset perturbation level of theory using the PT2F method[12a] included in *MOLCAS-3*[12b] with an augmented CAS with six electrons in 12 π orbitals.

The *cis* → *trans* isomerization and reactant back-formation paths are computed in two steps. In the first step, we compute the MEP describing the S_1 relaxation from the FC region of our system. This MEP is unambiguously determined by using a new methodology[27] to locate the initial direction of relaxation (IRD) from the starting point (i.e., the *cis*-$C_5H_6NH_2^+$ FC point). Briefly, an IRD corresponds to a local steepest descent direction, in mass-weighted cartesians, from a given starting point. The IRD is calculated by locating the energy minimum on a hyperspherical (i.e., $n-1$ dimensional) cross-section of the n dimensional potential energy surface centered on the starting point (n is the number of vibrational degrees of freedom of the molecule). The radius of this hypersphere is usually chosen to be small (typically ca. 0.25−0.5 au in mass-weighted cartesians) in order to locate the steepest direction in the vicinity of the starting point (i.e., the hypersphere center). The IRD is then defined as the vector joining the starting point (i.e., the center of the hypersphere) to the energy minimum. Once the IRD has been determined, the MEP is computed as the steepest descent line in mass-weighted cartesians using the IRD vector to define the initial direction to follow. As we will discuss below, a twisted conical intersection structure (i.e., a S_1/S_0 real crossing) point has been located by simply following the resulting downhill S_1 MEP until the S_1 and S_0 energies become degenerate. In the second step, we compute the MEPs describing the S_0 relaxation processes from the twisted S_1/S_0 conical intersection point (this is a highly unstable point, essentially a singularity, on the S_0 energy surface) determined in the first step. These MEPs are determined with the same methodology choosing the intersection point as the starting point. There are two such IRDs: the first connects the intersection point to the product (*all-trans*-$C_5H_6NH_2^+$) S_0 energy well and the second connects the intersection point to reactant (*cis*-$C_5H_6NH_2^+$) S_0 energy minimum.

The changes in bonding along the computed S_1 MEP have been documented using concepts derived from valence bond (VB) theory. Examples of this approach are given in reference 28a−c. The precise nature of the algorithm used in this work is given in the Appendix and is also discussed in a different context in ref 28d. Briefly, the six bonding and antibonding π molecular orbitals which result from a MC−SCF computation are localized using the Boys localization procedure available in *Gaussian 94*.[11b] The resulting localized orbitals are just the six "p atomic orbitals" forming an atomic orbital basis "AO" of the π-system of the molecule. In this localized "AO" basis the CI expansion (of the CAS) becomes a VB wave function consisting of covalent and ionic terms. The diagonal elements of the first order density matrix (which we shall refer to as D_{ii}) and the elements of the spin exchange density matrix defined in the appendix (which we shall refer to as P_{ij}) provide information on the occupancy of each "AO" and on the spin coupling between each pair (ij) of "AO", respectively. Since each "AO" resides on a different carbon or nitrogen center of the $C_5H_6NH_2^+$ backbone, this information can be used to derive the valence bond resonance formulae which best describe the bonding status of the system. A more detailed discussion is given in the next section.

3. Results and Discussion

The evolution of *cis* $C_5H_6NH_2^+$ along the MEP connecting the FC structure of the *cis* isomer to the S_0 *trans* and *cis* product wells is illustrated in Figure 1.

The S_1 state of *cis* $C_5H_6NH_2^+$ is ionic ^1B_u-like, whereas the S_1 energy surface of the corresponding polyene[29] *tZt*-hexa-1,3,5-triene is the covalent ^2A_g state. Along this path the energy difference between the S_1 and S_2 (covalent ^2A_g-like) states is large (>25 kcal mol^{-1}), and thus it appears that covalent S_2 is not involved in the reaction. The S_1 relaxation path ends at a point where the S_1 (^1B_u-like) and S_0 potential energy surfaces cross at a conical intersection (CI). The intersection point (CI)

(25) Michl, J.; Bonacic-Koutecky, V. *Electronic Aspects of Organic Photochemistry*; Wiley: New York, 1990.

(26) Bernardi, F.; Olivucci, M.; Robb, M. A. *Chem. Soc. Rev.* **1996**, *25*, 321.

(27) (a) Celani, P.; Robb, M. A.; Garavelli, M.; Bernardi F.; Olivucci, M. *Chem. Phys. Letters* **1995**, *243*, 1−8. (b) Garavelli, M.; Celani, P.; Fato, M.; Bearpark, M. J.; Smith, B. R.; Olivucci, M.; Robb, M. A. *J. Phys. Chem.* **1997**, *101*, 2023.

(28) (a) Bernardi, F.; Celani, P.; Olivucci, M.; Robb, M. A.; Suzzi-Valli, G. *J. Am. Chem. Soc.* **1995**, *117*, 10531−10536. (b) Bearpark, M. J.; Bernardi, F.; Olivucci, M.; Robb, M. A. *Int. J. Quantum Chem.* **1996**, *60*, 505−512. (c) Bearpark, M. J.; Bernardi, F.; Olivucci, M.; Robb, M. A.; Smith, B. R. *J. Am. Chem. Soc.* **1996**, *118*, 5254−5260. (d) Bearpark, M. J.; Robb, M. A.; Bernardi, F.; Olivucci M. *Chem. Phys. Lett.* **1994** *217* 513−519. (e) Pauncz, R. *Spin Eigenfunctions* Plenum Press: New York, 1979. (f) Bernardi, F.; Olivucci, M.; McDouall, J. J. W.; Robb, M. A. *J. Chem. Phys.* **1988**, *89*, 6365−6375.

(29) Olivucci, M.; Bernardi, F.; Celani, P.; Ragazos, I. N.; Robb, M. A. *J. Am. Chem. Soc.* **1994**, *116*, 1077−1085.

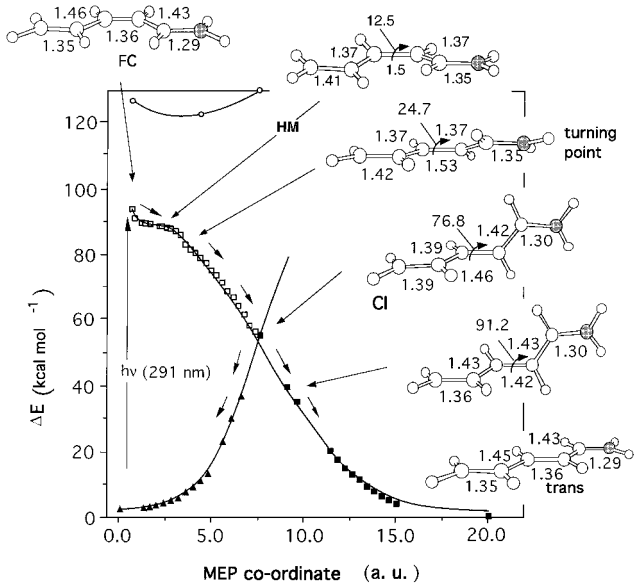

Figure 1. Energy profiles along the three MEPs describing the relaxation from the FC and CI points. Open squares and full squares curves define the excited (^1B_u-like) and ground state branches of the *cis* → *trans* photoisomerization path. Full triangles define the ground state *cis* back-formation path. Open circles show the dark (^2A_g-like) state energy along the excited state branch of the photoisomerization path. The energies of all points have been scaled to match the PT2F energies of the initial and final MEP points (see Table 1). The structures (geometrical parameters in angstroms and degrees) document the geometrical progression along the photoisomerization path.

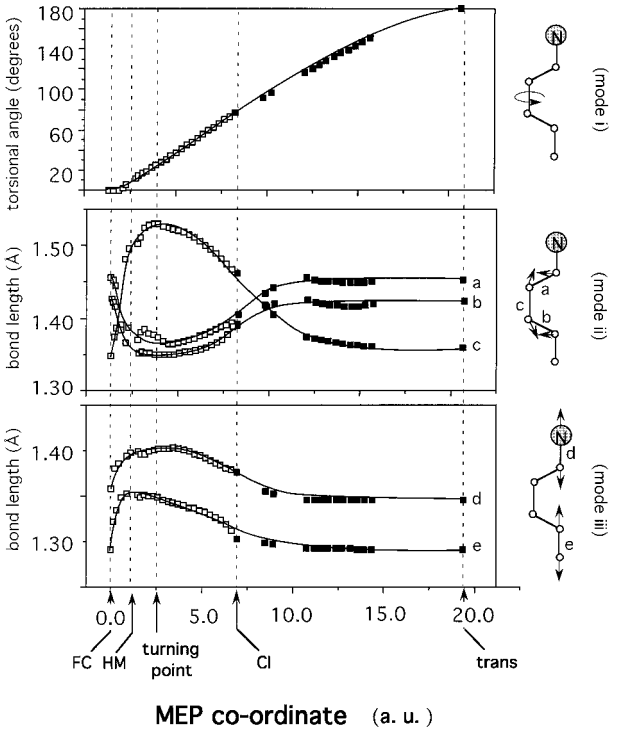

Figure 2. Reaction coordinate analysis along the excited (^1B_u-like) and ground state branches of the *cis* → *trans* photoisomerization MEP (see Figure 1) connecting *cis*-$C_5H_6NH_2^+$ (FC) to *trans*-$C_5H_6NH_2^+$ (trans).

has a ∼80° twisted central double bond which provides a route for fully efficient nonadiabatic *cis* → *trans* isomerization. Starting from this point, we have located two S_0 relaxation paths. The first path is a continuation of the excited state path and ends at the *all-trans* $C_5H_6NH_2^+$ well. The second path describes the back-formation of the reactant.

The *direct continuation* of the S_1 path on the ground state (through the CI point) is reflected by the smooth change in molecular structure along the entire photoisomerization coordinate (i.e., from the initial FC structure to the final *trans* $C_5H_6NH_2^+$ structure) and the corresponding change in the charge distribution. These points will be discussed in subsections i and ii, respectively. In the remaining three subsections, we discuss in more detail the properties of the S_1 branch of the isomerization pathway. In particular, in subsection iii, we present a valence bond analysis and interpretation of the change in bonding along the reaction coordinate. In subsection iv, we report few preliminary results on the effect of α-methyl substitution on the S_1 energetics, and finally, in subsection v, we discuss the generalization of the computed isomerization mechanism to longer PSB.

(i) Changes in Molecular Structure along the Reaction Coordinate. The *cis* → *trans* isomerization coordinate is documented in Figures 1 and 2. It is clear that the *cis* → *trans* isomerization coordinate is a combination of three coupled modes (see Figure 2): (i) twisting about the central double bond, (ii) symmetric stretching of the central -CH−CH=CH−CH- fragment, and (iii) in-phase stretching of the CH_2=CH- and -CH=NH_2^+ terminal fragments.

The reaction coordinate analysis of Figure 2 shows that the initial S_1 relaxation (from 0.0 to 1.5 au along the MEP coordinate) results in a substantial lengthening of all "formal" C−C double bonds rather than *cis* → *trans* twisting. While this bond expansion involves motion along both totally symmetric modes ii and iii, the excited state energy gradient at the FC structure (Figure 3a) indicates that the very initial acceleration must occur along mode iii which involves the C=N stretching and the stretching of the terminal C=C bond.

Thus, in *cis*-$C_5H_6NH_2^+$ the *cis* double bond expansion (mode ii) and isomerization (mode i) are not impulsive. Since this is an important point for the discussion of the relaxation dynamics of PSB, we have carefully determined the structure of the S_1 force field in the vicinity of the FC point. This has been achieved by using the IRD optimization method described in section 2 to probe the force field at different distances (0.25, 0.5, 0.75, 1.0, and 1.5 au) from FC.[30] As illustrated in Scheme 1, the energy minima (open squares) on the (hyper)spherical cross-sections at 0.25−1.0 au are located at untwisted (i.e., totally symmetric) structures. This clearly indicates that in this region the potential energy surface has the shape of a stable valley. This observation has been verified by demonstrating that small torsional deformations at the FC and the following points produce an energy increase. In contrast, the hypersphere energy minimum at the 1.5 au cross-section corresponds to a ca. 12° twisted structure (HM), indicating that the potential energy surface at this distance has the shape of an unstable energy ridge.

The type of coordinate described above is consistent with the presence of a bifurcation point[31] (BP) slightly beyond the point at 1.0 au as shown in Scheme 1. In fact, the planar structures optimized at 0.25, 0.5, 0.75, and 1.0 lie on the steepest descent line computed starting from the FC point. However, this line does not pass through the twisted minimum HM but continues along the planar structures[30] located along the unstable

(30) In this region, the standard methods for computing steepest descent lines would fail to locate the correct relaxation path (e.g., these methods usually retain the symmetry of the initial structure). Accordingly, for this region, we have computed the MEP using a computational strategy based upon a series of IRD optimizations performed at increasing values of the distance (radius of the hypersphere) from the starting point.

(31) Schlegel, H. B. *J. Chem. Soc., Faraday Trans.* **1994**, *90*, 1569−1574.

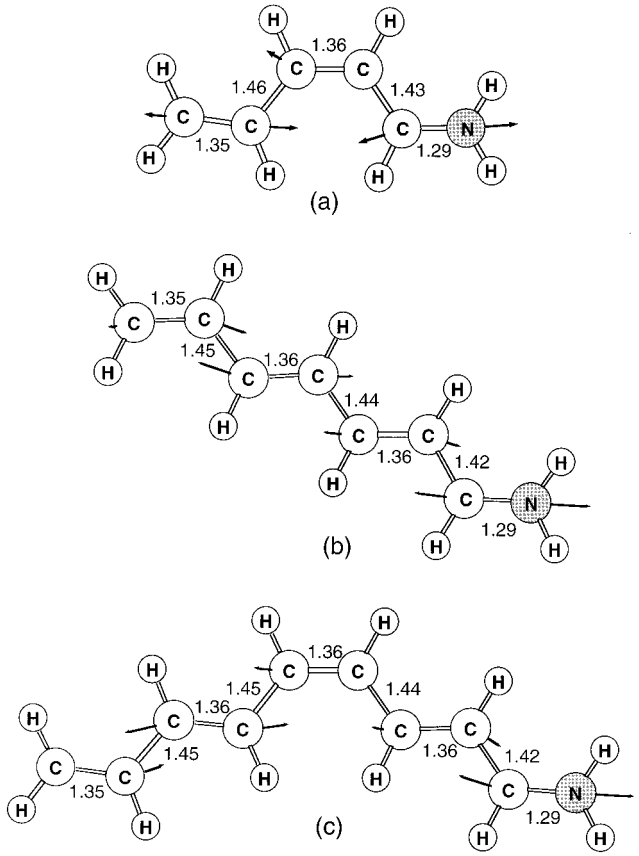

Figure 3. Ground state equilibrium structure (relevant geometrical parameters in angstroms) and excited state energy gradient vectors for (a) *cis*-$C_5H_6NH_2^+$, (b) *all-trans*-hepta-3,5,7-trieneimine cation (see Table 2 for details), and (c) *tEtZtEt*-nona-3,5,7,9-tetraenimine cation (optimized at the MC−SCF level of theory with a CAS with 10 electrons in 10 orbital and 6-31G* basis set). The arrows in the FC structures represent the direction of the force vector (i.e., −grad).

Scheme 1

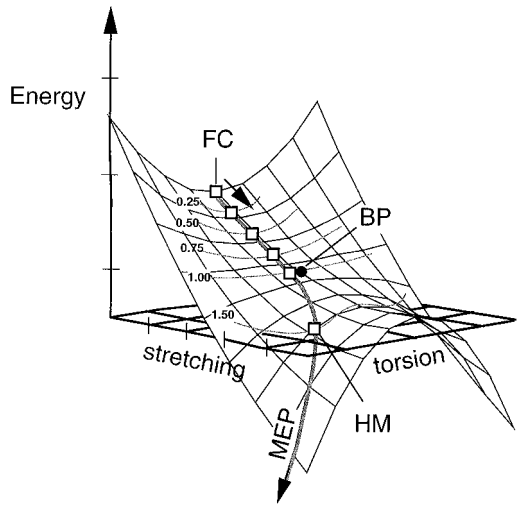

energy ridge of Scheme 1. In order to define the "whole" S_1 isomerization coordinate, we compute a second steepest descent line starting at the 12° twisted point HM. Thus, our S_1 MEP coordinate (Figures 1 and 2) follows, by definition, the steepest descent line starting at FC up to a distance of 1.0 au, "avoids" the bifurcation point BP, and then "continues" along the steepest descent path starting at HM.

While the initial acceleration corresponds, as discussed above, to mode iii, this type of deformation changes rapidly along the relaxation coordinate, and already at 1.0 au along the MEP

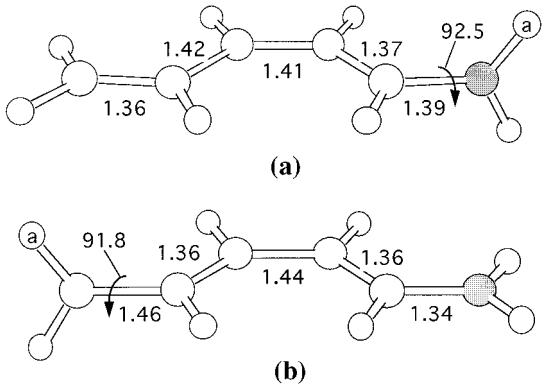

Figure 4. Molecular structure and relevant geometrical parameters (angstroms and degrees) for (a) the twisted -NH_2^+ S_1 minimum (angle given for the H_a−N−C−C torsion) and (b) the twisted -CH_2 S_1 minimum (angle given for the H_a−C−C−C torsion).

coordinate, mode ii has strongly mixed with mode iii leading to a large expansion of the *cis* double bond and contraction of the two adjacent bonds. It is clear from Figure 2 that at 1.0 au the expansion along mode iii is completed and the stretching motion becomes dominated by mode ii. Beyond this point, the torsional deformation begins, and at 1.5 au (corresponding to the ca. 12° twisted HM structure with a 1.50 Å expanded *cis* double bond), the stretching along mode ii is strongly mixed with mode i. The stretching along mode ii terminates at a "turning point" where the molecule has a 1.53 Å expanded central double bond but is only 25° twisted. From this point on, the stretching deformations invert and the twisting of the central double bond becomes dominant. Very remarkably, the S_1 branch of the isomerization coordinate (open squares) correlates nicely with the S_0 branch (full squares) demonstrating that the S_1 relaxation coordinate *continues* on the ground state.

The S_1 isomerization about the terminal -CH=NH_2^+ and CH_2=CH- double bonds has also been investigated. These processes lead to two twisted S_1 minima whose structures are reported in Figure 4. As apparent from Table 1, these minima are located in regions lying >25 kcal mol^{-1} above the CI structure and where the S_1 and S_0 energy surfaces are >30 kcal mol^{-1} avoided.

(ii) Changes in Charge Distribution along the Reaction Coordinate. Figure 5 shows the evolution of the Mulliken charges[32] (with hydrogens summed into heavy atoms) along the reaction coordinate. The *cis* $S_0 \rightarrow S_1$ FC excitation results in a partial single-electron transfer toward the NH_2 end of the molecule, which is consistent with the charge transfer associated with the HOMO−LUMO singly excited ^1B_u-like nature of S_1.[13,15] Accordingly, the positive charge migrates toward the -CH_2 molecular end. The most striking feature is the large, but regular, increase (from ca. 0.0 to +0.39) of the charge at the γ carbon center along the S_1 path. This center is adjacent to the rotating bond and a stabilization of its positive charge must have an important effect on the stability of the twisted configuration.

Along the isomerization coordinate, the excited state charge distribution is smoothly changed, and this change continues into the ground state branch of the reaction (i.e., after CI) where the positive charge is shifted back toward the -NH_2 molecular end.

(32) (a) Atomic charges computed using three additional schemes (NPA,[32b] CHelpG,[32c] MKS[32d]) yield the same charge distribution. Thus, in Figure 5 we report Mulliken charges only. (b) Computed with the program: *NBO* Version 3.1, Glendening, E. D.; Reed, A. E. Carpenter, J. E.; Weinhold, F. See also: Reed, A. E.; Weinhold, F. *J. Am. Chem. Soc.* **1980**, *102*, 7211). (c) See: Breneman, C. M.; Wiberg, K. B. *J. Comput. Chem.* **1990**, *11*, 361. (d) See: Besler, B. H.; Metz, K. M., Jr.; Kollman, P. A. *J. Comput. Chem.* **1990**, *11*, 431.

Table 1. Multireference Perturbation Theory (PT2F) and MC−SCF (in brackets) 6-31+G* Relative (ΔE) Energies[a]

structure		ΔE[b] (kcal mol^{-1})
cis-$C_5H_6NH_2^+$ S_0 MIN		
	S_0	3.5
		(3.39)
	S_1	96.1
		(108.9)
	S_2	127.3
trans-$C_5H_6NH_2^+$ S_0 MIN		
	S_0	0.0
		(0.0)
	S_1	95.1
		(110.5)
CI[c]		
	S_0	56.3
		(62.1)
	S_1	53.9
		(64.8)
	S_2	131.8
CI optimized[d]		
	S_0	54.3
		(59.6)
	S_1	51.2
		(61.7)
twisted NH_2^+ S_1 MIN		
	S_0	46.0
		(52.6)
	S_1	78.5
		(92.6)
twisted CH_2 S_1 MIN		
	S_0	55.3
		(70.5)
	S_1	89.9
		(91.7)
α-methyl-*cis*-$C_5H_6NH_2^+$ S_0 MIN[e]		
	S_0	0.0
		(0.0)
	S_1	97.0
		(114.7)
	S_2	126.4
		(136.6)

[a] See Supporting Information for absolute energy values. [b] All energy values are computed using state-averaged orbitals and a CAS with six electrons in 12 orbitals. [c] This structure corresponds to the last optimized point along the S_1 (*cis* → CI) MEP. [d] The lowest energy crossing point has also been located (using state-averaged orbitals to avoid root-flipping problems). It is found that this point corresponds to the absolute energy minimum of the S_1 state. The corresponding structure is only slightly different from structure CI and <3 kcal mol^{-1} more stable. This structure corresponds to the absolute minimum found on the S_1 potential energy surface. The <3 kcal mol^{-1} S_1-S_0 energy gap computed at the PT2F level is due to the accuracy of the method and to the fact that the structure is optimized in absence of dynamic correlation effects. [e] The basis set used here is 6-31G*.

As shown in Figure 5, in the vicinity of the CI point about 70% of the positive charge is localized on the allyl fragment due to depopulation of its singly occupied molecular orbital (SOMO).

The fact that the charge migration along the S_1 coordinate reaches its maximum at the highly twisted CI structure may be connected with the phenomenon generally referred to as "sudden polarization", which has been extensively studied by Salem.[33] However, it must be noticed that in *cis*-$C_5H_6NH_2^+$ the increase in polarization along the computed MEP is gradual and a polarization corresponding to the migration of ca. 0.5 electron toward the -CH−CH=NH_2 is already present in the untwisted FC region. Thus, this case is remarkably different from the case of *tZc*-hexatriene where the polarization of the molecule (in its ionic excited state) occurs suddenly when the molecule is nearly completely twisted.[33b]

(33) (a) Salem, L.; Bruckmann, P. *Nature* **1975**, *258*, 526−528. (b) Salem, L. *Acc. Chem. Res.* **1979**, *12*, 87−92.

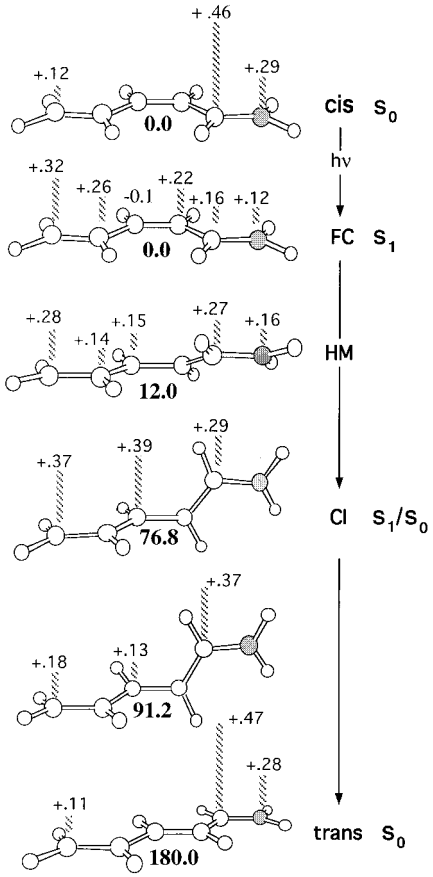

Figure 5. Evolution of the charge distribution along the excited (^1B_u-like) and ground state branches of the *cis* → *trans* photoisomerization MEP (see Figure 1) connecting *cis*-$C_5H_6NH_2^+$ (FC) to *trans*-$C_5H_6NH_2^+$ (**trans**). The charges are given in au, and the value of the central torsional angle is given in degrees.

(iii) Changes in Bonding along the Reaction Coordinate. While the MEP presented in Figure 1 provides a "structural" description of the isomerization process, the nature of the changes on bonding becomes evident using VB theory. As mentioned in section 2, we have recently implemented a method (see ref 28 and the Appendix) which allows for a quantitative valence bond analysis of the wave function along the reaction coordinate. The valence bond analysis of the wave function at any point along the reaction path yields the bonding (or antibonding) status of each pair of centers along the π system. This status is given by the numerical value of the spin exchange density matrix elements P_{ij} where *i* and *j* are the two centers (or, more precisely, the pair of π "AO" residing on centers *i* and *j*). The P_{ij} have real values in the range between +1 and −1. A positive value close to +1 indicates that center *i* and *j* are singlet spin coupled (i.e. *bonding*). In contrast, a value between 0 and −1 indicates that the centers are either uncoupled (−0.5 if *i* and *j* are each fully coupled in a different pair such as *ik* and *jl*) or triplet spin coupled (−1) (i.e., *antibonding*). Well-defined force fields can be associated with pairs of *bonding* and *antibonding* centers. These are illustrated in Scheme 2 for but-2-ene.[34] In this molecule, the π system corresponds to a single double bond and the P_{ij} has only two possible values: +1 for the S_0 energy surface where the two π electrons are bonded and −1 for the T_1 energy surface where the electrons are antibonded. While the force field for S_0 has its minimum at a planar configuration with a short 1.34 Å bond length, the

(34) These surfaces have been computed using *ab initio* MC−SCF theory with a 6-31G* basis set. We are grateful to Dr. Barbara Frabboni for providing these data.

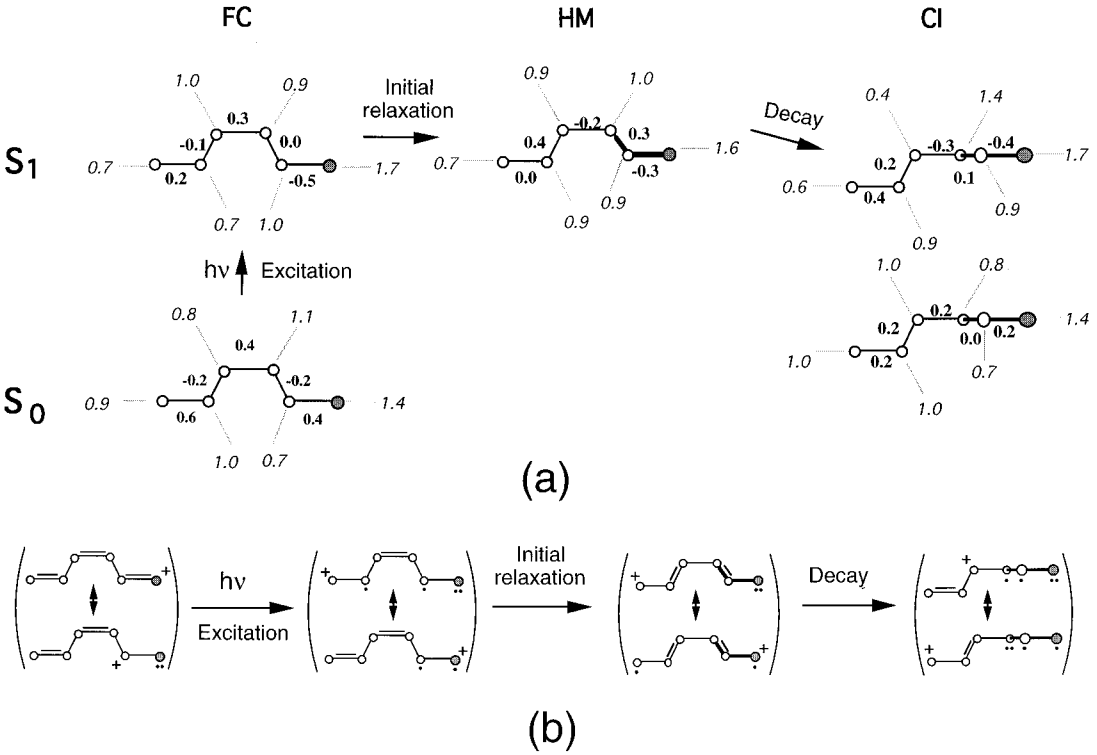

Figure 6. Valence bond wave function analysis of the bonding status along the S_1 MEP describing the relaxation from *cis*-$C_5H_6NH_2^+$ (FC) to the conical intersection point (CI). At the CI structure the S_0 and S_1 states are degenerate. (a) P_{ij} (bold) and D_{ii} (italic) values for S_0 *cis*-$C_5H_6NH_2^+$ and for three structures (FC, HM, CI) along the S_1 MEP. (b) Resonance formulas describing the bonding of the four structures analyzed in a.

Scheme 2

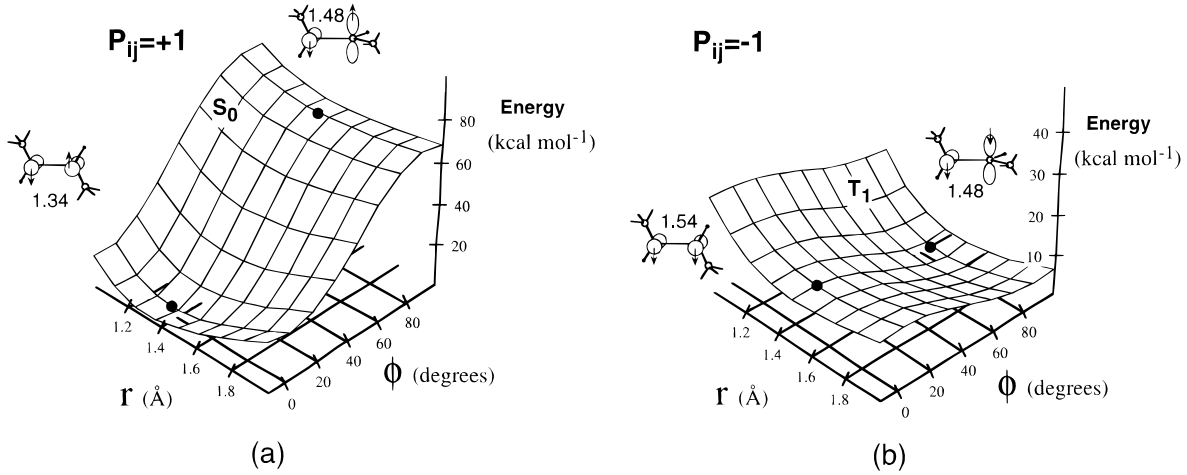

T_1 force field has its minimum at a twisted configuration where the two π electrons do not interact. However, notice that at planar configurations the T_1 force field has its minimum at a very long bond distance of 1.54 Å due to repulsion of the π electrons.

In Figure 6a we present the results of our wave function analysis at four relevant points along the excited state MEP coordinate. One can easily recognize three major changes. The first change occurs in the photoexcitation step at the ground state equilibrium structure. In the ground state structure, the positive P_{ij} values are located at the "formal" double bonds. The values of the diagonal elements of the first-order density matrix (D_{ii}) indicate that there is roughly one electron on each center (with the exception of the C═N bond which is polarized toward the N atom so that D_{ii} on the C atom is 0.7 and D_{ii} on the N atom is 1.4). After the absorption of the photon, the P_{ij} value at the C═N bond assumes a large and negative value, and the terminal C═C P_{ij} is strongly reduced in value. In contrast, the central C═C double bond remains substantially bonding. This bonding pattern explains the gradient direction seen in Figure 3a and the dominance of mode iii (Figure 2), which corresponds to stretching of the C═N and terminal C═C bonds, in the initial part of the S_1 path. The large and positive P_{ij} at the central double bond also indicates that at the FC geometry the system will be initially stable with respect to twisting motion (consistent with the potential in Scheme 2a) *so that there is no tendency to initiate cis → trans isomerization motion*. The S_1 electron density at FC geometry shows an ca. 0.5 electron increase on the C−N moiety and a corresponding decrease on the terminal C−C fragment. This is consistent with the change in charge distribution seen in Figure 5.

The second change occurs soon after the system leaves the FC point via stretching motions (see subsection i). It is clear from the P_{ij} values at structure HM (i.e., at 1.5 au along the MEP) that a dramatic change in bonding has occurred corresponding to a change from a *bonding* to an *antibonding* status

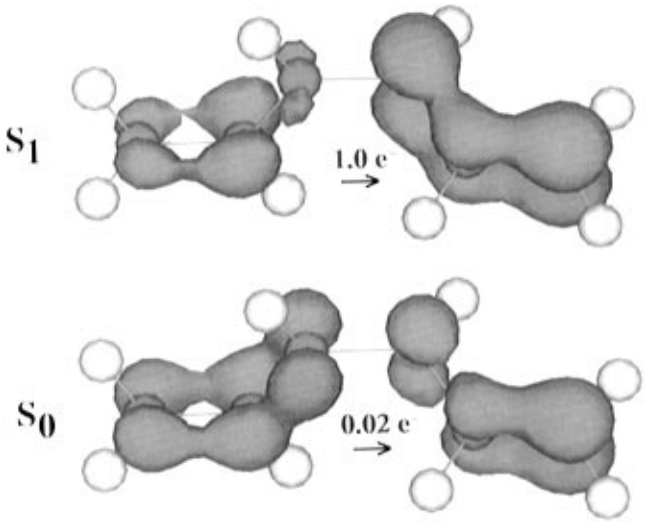

Figure 7. Plot of the π electron density for the degenerate S_0 and S_1 states at the conical intersection structure (CI). The arrows indicate the number of electrons migrated from the CH_2CHCH- allyl fragment to the -$CHCHNH_2$ fragment.

of the central double bond. There is no dramatic change of the electron density, but rather simply a change in spin coupling. The new P_{ij} pattern indicates that the force field of the central double bond is now very similar to that of Scheme 2b. Therefore, the system must be now *unstable* with respect to the central double bond twisting and a small (ca. 12°) rotation is already present at this point together with a large bond length stretching to 1.50 Å. This change in bonding rationalizes the mixing of modes ii and iii in the initial part of the S_1 MEP and the reaction coordinate bifurcation (see Scheme 1) and explains the creation of an unstable central double bond. This change is summarized by the resonance structures given in Figure 6b.

The third change occurs along the relaxation from the turning point structure to the CI structure and involves an additional 0.5 electron transfer toward the C−N end of the molecule. As a result of this transfer the S_1 relaxation of *cis*-$C_5H_6NH_2^+$ results in a *net* one-electron transfer from the allyl to the -CH−CH−NH_2 molecular fragment. This is also demonstrated in Figure 7. Here, we show the π-electron density in S_0 and S_1 at the conical intersection structure.

The existence of a conical intersection point and the charge motion observed along the computed isomerization coordinate can be rationalized using the "two-electron two-orbital model" of Michl and Bonacic-Koutecky et al.[18b,25] According to this theory, the twisted CI structure corresponds to a "critically heterosymmetric biradicaloid". A heterosymmetric biradicaloid is a structure where two localized orbitals have different energies but do not interact. This is the situation found in the CI structure presented above where one has that the SOMO π orbital of the allyl fragment and the SOMO π orbital of the -$CHCH_2NH_2^+$ fragment are not overlapping. In this condition, the energy separation of the "ionic" S_1 and "covalent" S_0 states depends on the difference between the electron affinity of the allyl SOMO and the ionization potential of the -$CHCH_2NH_2^+$ SOMO. These quantities can be changed as a function of the fragment structure. Thus, along the last part of the S_1 reaction coordinate, the geometry of the two fragments is such that these energies become equal. Consequently, the S_1 energy is lowered, and ultimately, the S_1 surface crosses with the S_0 surface. This interpretation is strongly supported by the π electron densities for the degenerate S_0 and S_1 states reported in Figure 7.

(iv) Effects of α-Methylation. As reported in eq 1, PSB11 has a methyl group at the C_{13} position. Therefore, nonbonded interaction between the C_{13}-methyl group and the C_{10}-hydrogen may be important in triggering the isomerization process. Recent work by Mathies et al. on 13-demethylrhodopsin[35] (a protein which contains a 13-demethyl PSB11 chromophore) has clearly revealed that methylation increases the reaction rate of a factor of 2 and also induces a 3-fold increase in the isomerization quantum yield. Because our model represents a gross simplification of the 13-demethylrhodopsin chromophore, some exploratory computations have been carried out to probe the sensitivity of the initial S_1 MEP to the presence of an α-methyl substituent. In Figure 8, we compare the molecular structure and S_1 energy gradient at the FC point of the α-methyl-substituted and unsubstituted *cis*-$C_5H_6NH_2^+$. While the gradients are very similar, it must be observed that the substituent induces a larger component along the central double bond stretch. This component must increase the rate of change in spin coupling required for making the central double bond torsionally unstable (see discussion above). In fact, as reported in the same figure, α-methyl substitution leads to a ca. 2-fold increase of the very initial slope of the S_1 MEP. In fact, while the molecular structure at 1.5 au (point HM) is the same for both the substituted and unsubstituted PSB, the former is two times more stable (relative to the FC point).

Table 2. State-Averaged[a] and Single State[b] (in parenthesis) MC−SCF 6-31G* Relative (ΔE) Energies[a]

structure		ΔE (kcal mol^{-1})
trans-$C_7H_8NH_2^+$ S_0 MIN		
	S_0	0.0
		(0.0)
	S_1	92.2
		(97.3)
$CI_{\beta-\gamma}$[d]		
	S_0	53.1
	S_1	60.6
$CI_{\delta-\epsilon}$[d]		
	S_0	63.0
		(54.1)
	S_1	64.8
		(58.5)

[a] All values are computed using root 1 and root 2 state-averaged orbitals and a CAS with eight electrons in 12 orbitals. [b] All values are computed using a CAS with eight electrons in eight orbitals. [c] This crossing point has been located (using state-averaged orbitals to avoid root-flipping problems) empirically. A rigorous optimization of these structures is now in progress.

(v) Generalization to Longer PSB. One of the most important questions to be answered by future work concerns the generalization of the results reported in subsections i−iv to the PSB11 rhodopsin chromophore (see eq 1). Encouraging indications on the general validity of the above mechanistic picture come from the results presented in Table 2 and Figure 9 for the *all-trans*-hepta-3,5,7-trieniminium cation where the chain length has been extended by one ethylene unit.

In this molecule, two fully twisted conical intersection points have been identified which correspond to rotation about the two central $C_\beta-C_\gamma$ ($CI_{\beta-\gamma}$ in Figure 9a) and $C_\delta-C_\epsilon$ ($CI_{\delta-\epsilon}$, in Figure 9b) bonds of the molecule. These structures (given in Figure 4a,b) lie 28 and 32 kcal mol^{-1} below the FC structure, respectively. The expected decrease in energy separation between the conical intersection and the FC point reflects the increase in length of the π system. Additional evidence supporting an invariant topology for the S_1 energy surface of PSB for different chain lengths comes from the comparison of

(35) (a) Wang, Q.; Kochendoerfer, G. G.; Schoenlein, R. W.; Verdegem, P. J. E.; Lugtenburg, J.; Mathies, R. A.; Shank, C. V. *J. Phys. Chem.* **1996**, *100*, 17388−17394. (b) Schoenlein, R. W.; Peteanu, L. A.; Wang, Q.; Mathies, R. A.; Shank, C. V. *J. Phys. Chem.* **1993**, *97*, 12087−12092.

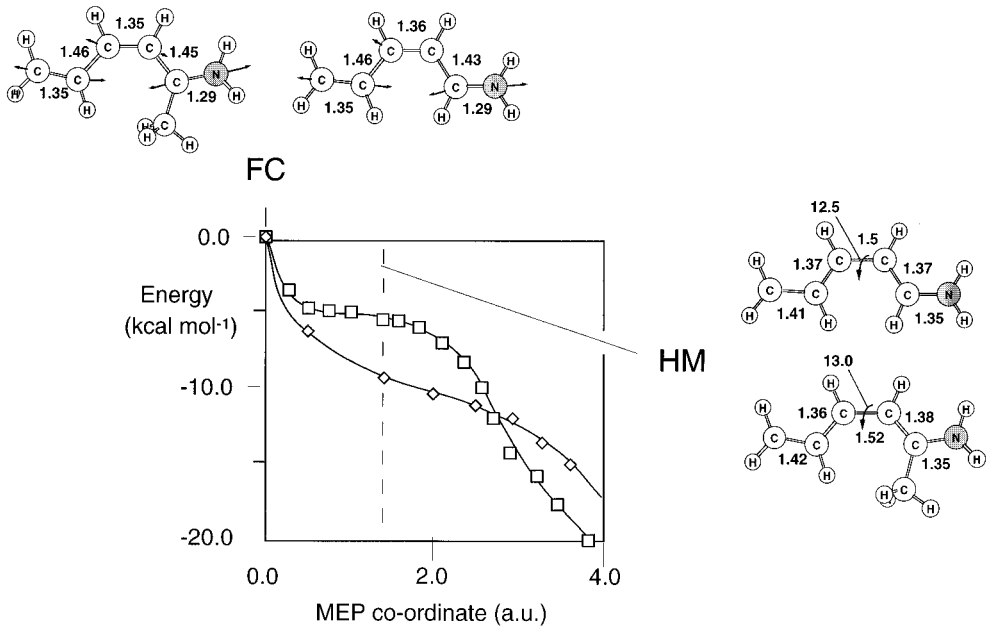

Figure 8. Comparison of the molecular structures, energy gradient, and S_1 MEP initial energy profiles for *cis*-$C_5H_6NH_2^+$ (open squares) and α-methyl *cis*-$C_5H_6NH_2^+$ (open diamonds). The relevant geometrical parameters are given in angstroms and degrees. The arrows in the FC structures represent the direction of the force vector (i.e., −grad). The structures at a 1.5 au distance from the FC point are indicated by the label HM.

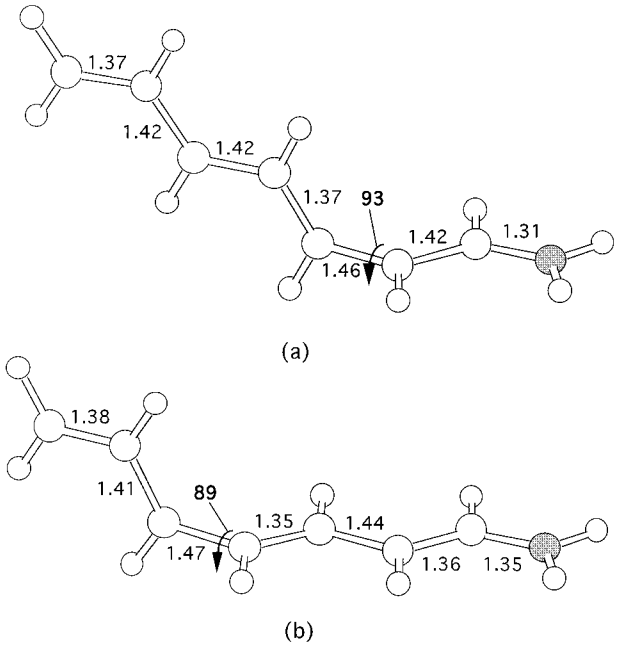

Figure 9. Molecular structure and relevant geometrical parameters (angstroms and degrees) for (a) a $C_\beta-C_\gamma$ S_1/S_0 conical intersection and (b) a $C_\delta-C_\epsilon$ S_1/S_0 conical intersection.

the excited state energy gradients. As shown in Figure 3b,c, at the FC structure both the *all-trans*-hepta-3,5,7-trieniminium and *tEtZtEt*-nona-3,5,7,9-tetraeniminium cations show a direction and magnitude of the energy gradient which is very similar to that seen in Figure 3a for our minimal model. In both cases, the initial -C═N stretching motion dominates while the $C_\beta-C_\gamma$ and $C_\delta-C_\epsilon$ stretches in the heptatrieniminium and central double bond in the nonatetraenimminium cations show only minor components along the initial acceleration.

4. Conclusions

Our results demonstrate that a minimal but accurately computed model can provide potential energy surfaces and reaction paths consistent with the qualitative aspects of retinal (and rhodopsin) photoisomerization. First, the computed excited state relaxation path and the conical intersection provide a barrierless and fully efficient $S_1 \rightarrow S_0$ radiationless decay channel which is fully consistent with the observed short time scale of the *cis* → *trans* isomerization motion of PSB11.[2,4] The lack of excited state equilibration is consistent with the observation of coherent vibrational motion in the photoproduct population,[2b] and the oscillatory behavior should have components along the torsional (low-frequency) modes. Second, the computed structure of the S_1 isomerization coordinate implies that the initial relaxation motion is dominated by stretching modes which ultimately result in an elongation of the central double bond of the molecule. The actual *cis* → *trans* isomerization motion is induced only after considerable bond stretching. This feature of the excited state force field is consistent with the transient absorption spectra of rhodopsin reported by Shichida et al.[3] who suggest that during the first 25 fs the excited state PSB11 chromophore moves out of the FC region along a stretching mode and reaches a lower energy S_1 region where $S_1 \rightarrow S_0$ decay occurs within 60 fs. Third, α-methyl substitution in our minimal PSB leads to a 2-fold increase in the slope of the initial part of the computed S_1 isomerization path. Again, this appears to be consistent with the observed[35] increase in velocity and quantum yield of the *cis* → *trans* isomerization process in C_{13}-demethyl chromophores. Fourth, we have shown that a generalization of the *cis* → *trans* isomerization mechanism found in *cis*-$C_5H_6NH_2^+$ to longer PSB is supported by computations on the longer *all-trans*-hepta-3,5,7-trieniminium cation.

In Scheme 3, we now propose a general view of the two-dimensional structure of the S_1 potential energy surface of isolated polyenic PSB cations which seems to accommodate the present knowledge.

The *cis* → *trans* isomerization MEP spanning this surface (see stream of arrows) involves initial acceleration along a topologically stable valley starting at the FC point and dominated by totally symmetric stretching modes. Progression along these modes causes a change in the valley topology which becomes a ridge. As a result of this change, two equivalent new valleys (with components along both the stretching and the torsional modes) originate at a bifurcation point (BP). The actual *cis* →

Scheme 3

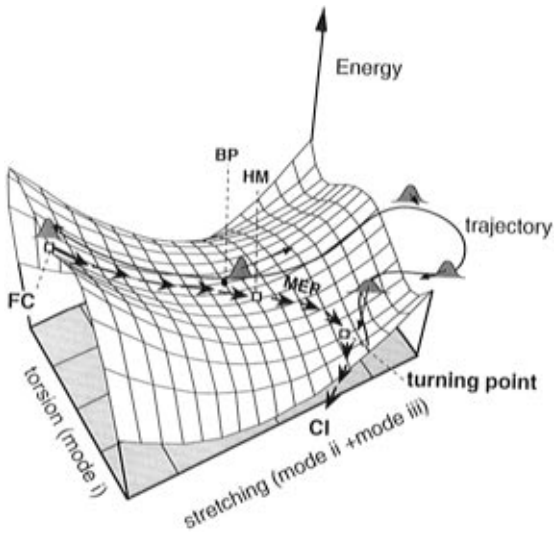

trans isomerization motion begins in these valleys and leads, ultimately, to the CI point where decay to S_0 occurs with a 100% efficiency. Remarkably, these valleys have a very large gradient because of the fully stretched and *antibonding* (i.e., $P_{ij} < 0$) central double bond near the HM point.

In order to estimate the time scale for the *cis* → *trans* isomerization dynamics, the whole nonadiabatic path of Figure 1 has been modeled as a one-dimensional motion of a particle of proper reduced mass.[36] This crude model should provide an estimate of the lower-limit time scale as the particle is forced to move along the computed isomerization coordinate. According to our estimate the photoexcited molecule reaches the region of the double bond stretching turning point in ∼35 fs, the CI point is reached after ∼55 fs and the *trans* well after ∼90 fs. Wave packet dynamics (initiated by ultrashort laser pulses) will not follow the S_1 MEP branch reported in Figure 1 and Scheme 3. Rather, after the initial acceleration, the motion of the wave packet would be expected to continue along the stretching coordinate well beyond the BP point.[37] This motion will, presumably, bring the system in a very unstable region of the surface where the bonds are highly stretched. In this region, the wave packet will have little kinetic energy and will then start the *cis* → *trans* isomerization motion toward the bottom of the energy surface, as illustrated in Scheme 3. As mentioned above, this motion seems to be consistent with the dynamics view proposed by Shichida et al.[3] for explaining the presence of a "fluorescent state" reached ca. 25 fs after excitation and that proposed by Mathies et al.[2] for explaining the observation of vibrational coherence in rhodopsin.

As discussed in the Introduction, our model does not include solvent, cavity, or counterion. Thus, the qualitative features discussed above *are predicted to be intrinsic to polyenic protonated Shiff bases*. This prediction must be relevant to the general mechanism of PSB11 photoisomerization in rhodopsin. For instance, the *cis*-$C_5H_6NH_2^+$ and *all-trans*-hepta-3,5,7-trieniminium cation suggest that there is a driving force for preferential single bond isomerization *at the center* of the molecular chain. This implies that, in a longer chain, the double bonds in the middle of the chain will isomerize much more efficiently. Thus, in PSB11 and in *all-trans*-PSB one expects competitive isomerization at the 9, 11, and 13 positions with preferential isomerization at the 11 position. This is consistent with the quantum yield values for both the *cis* → *trans* and *trans* → *cis* photoisomerization of retinal in solution.[13] The structure of the computed reaction path suggests that there is no driving force for a bicycle pedal *cis* → *trans* isomerization motion[38] (outside of a molecular cavity) but that the isomerization occurs via a single torsional motion. Therefore, the *cis* → *trans* isomerization mode in protonated Shiff bases is very different from the one found in polyenes[10] (including *tZt*-hexa-1,3,5-triene[27]) where at least two adjacent torsional modes are involved in the S_1 motion (this is also discussed in ref 19). This difference is certainly related to the difference in the electronic nature of the S_1 state which is covalent (A_g) in polyenes and ionic (B_u-like) in protonated Shiff bases.[15,17−19]

The evolution of the position of the protonated Shiff base positive charge along the computed isomerization path must be relevant to the issue of the control of PSB11 and PSBT photoisomerization rate, specificity, and quantum yield in rhodopsin and bacteriorhodopsin. Recently, there has been considerable speculation about the role of charged amino acids and in particular the carboxyl counterion in the photoisomerization efficiency.[39] From our computations, there is no doubt that, during the excited state motion, the positive charge is located along the polyenic (all-carbons) half of the twisting bond. Strategically placed counterions can thus select the bond which isomerizes. Such a control mechanism could explain quite well the behavior of PSBT in bacteriorhodopsin which isomerizes specifically to PSB13 (i.e., the 13-*cis* isomer of the retinal protonated Shiff base) even if in solution this photoproduct forms in a less extent than PSB11.[13] The effect of a strategically placed carboxyl counterion on the *cis*-$C_5H_6NH_2^+$ photoisomerization MEP of Figure 1 is now being investigated.

Acknowledgment. The authors thank R. A. Mathies and A. Warshel for helpful discussions. This research has been supported in part by the EPSRC (UK) under grant number GR/K04811, by an EU TMR network grant (ERB 4061 PL95 1290, Quantum Chemistry for the Excited State), and by the University of Bologna under grant number 908 and funds for selected research topics. We are also grateful to NATO for a travel grant (CRG 950748).

Supporting Information Available: Cartesian coordinates of all structures discussed in the text and listed in the tables, the D_{ii} and P_{ij} matrix element tables for the structures represented in Figure 6, and two tables (Table IS and IIS) containing the PT2F and MC−SCF absolute energies for the structures listed in Table 1 and 2 (12 pages). See any current masthead page for ordering and Internet access instructions.

Appendix: Valence Bond Analysis of MC−SCF Wave Functions using Spin Exchange Density Matrix Elements P_{ij}

The matrix elements of a valence bond Hamiltonian in the space of covalent (i.e., all of the spatial orbitals are singly occupied) determinants $|K\rangle$ and $|L\rangle$ can be written as (see for example ref 28d)

(36) The trajectory **s** is obtained by solving (numerically) the following equation of motion $\mathbf{m}(\mathbf{s})\cdot\mathbf{s}'' + (\mathbf{s}')^2\cdot d\mathbf{m}(\mathbf{s})/d\mathbf{s} = -d\mathbf{E}(\mathbf{s})/d\mathbf{s}$ where **s** is the photoisomerization coordinate and **m**(**s**) and **E**(**s**) are the corresponding effective reduced mass and potential energy along the composite MEP series of FC → IC → *trans*-product.

(37) This region of the S_1 surface has not been carefully characterized in this study, which mainly concentrates on MEPs. However, it seems that for *untwisted cis*-$C_5H_6NH_2^+$ configurations there is a flat region centered on stretched structures. The detailed topology of this region will be presented in a more technical paper.

(38) Warshel, A. *Nature* **1976**, *260*, 679−683.

(39) Zhang, H.; Lerro, K. A.; Yamamoto, T.; Lien, T. H.; Sastry, L.; Gawinowicz, M. A.; Nakanishi, K. *J. Am. Chem. Soc.* **1994**, *116*, 10165−10173.

$$H_{KL} = \delta_{KL}Q + \sum_{ij} B_{ijij}^{KL}K_{ij} \tag{A1}$$

where B_{ijij}^{KL} is defined as

$$B_{ijij}^{KL} = \langle K|a_i^+ a_j^+ a_j a_i|L\rangle \tag{A2}$$

and a_i^+ and a_j are annihilation and creation operators for spin orbitals i and j. The K_{ij} are the "exchange" integrals of Heitler−London VB theory that depend mainly on the overlap between spatial orbitals. The VB wave function is assumed to have the form

$$\Psi = \sum C_K|K\rangle \tag{A3}$$

The energy is given as

$$E = Q + \sum_{ij} P_{ij}K_{ij} \tag{A4}$$

where the P_{ij} are defined as

$$P_{ij} = \sum_{KL} C_K C_L \langle K|a_i^+ a_j^+ a_j a_i|L\rangle \tag{A5}$$

and the C_K are the VB wave function expansion coefficients.

For a MC−SCF wave function with a complete active space (CAS), localizing the active orbitals results in orbitals "AO" that are localized on atomic sites. Thus, the CAS configurations can now be interpreted as covalent or ionic VB configurations. As we illustrated elsewhere,[28a,f] the K_{ij} could be extracted from an effective Hamiltonian. However, the P_{ij} can be obtained directly from the CAS−SCF wave function in the localized orbital ("AO") basis without the need to compute an effective Hamiltonian. In the limit of a purely covalent wave function, diagonal elements, P_{ii} are 0. In real chemical systems, they are a measure of the ionicity of the electronic state.

In fact, the P_{ij} are a partition of the expectation value of the S^2 operator and are thus a fundamental property of the wave function.[28e] Thus, we have for n active electrons and N active spin orbitals

$$\langle\Psi|\hat{P}|\Psi\rangle = \langle\Psi|\sum_{\mu<\nu}^{n}(2\hat{S}(\mu)\cdot\hat{S}(\nu) + {}^1/_2\hat{I})|\Psi\rangle = S(S+1) + \frac{n(n-4)}{4} \tag{A6}$$

where $\hat{S}$ is the spin operator and $\hat{I}$ is the identity operator. In second quantization formalism, eq A6 can be written as

$$\langle\Psi|\sum_{\mu<\nu}^{n}(2\hat{S}(\mu)\cdot\hat{S}(\nu) + {}^1/_2\hat{I})|\Psi\rangle = \sum_{i,j,k,l=1}^{N}\langle i(1)j(2)|\sum_{\mu<\nu}^{n}(2\hat{S}(\mu)\cdot\hat{S}(\nu) + {}^1/_2\hat{I})|k(1)l(2)\rangle\langle\Psi|a_i^+ a_j^+ a a_k|\Psi\rangle \tag{A7}$$

and only the "exchange" density terms survive. For a CAS wave function, the orthogonality of α and β spatial orbitals allows further simplifications of eq A7. Eliminating the spin from eq A7, eq A6 can be written as

$$\langle\Psi|\hat{P}|\Psi\rangle = \sum_{r,s}^{M} P_{rs} \tag{A8}$$

where the sums run now on all of the M active spatial orbitals. The elements of the matrix in eq A8 are the values used in the paper.

JA9610895